Inelastic neutron scattering and lattice dynamical calculation of negative thermal expansion in HfW_2O_8

R. Mittal,[1] S. L. Chaplot,[1] A. I. Kolesnikov,[2] C.-K. Loong,[2] and T. A. Mary[3]
[1]*Solid State Physics Division, Bhabha Atomic Research Centre, Trombay, Mumbai 400 085, India*
[2]*Intense Pulsed Neutron Source Division, Argonne National Laboratory, Argonne, Illinois 60439, USA*
[3]*Materials Science, California Institute of Technology, Pasadena, California 91125, USA*
(Received 10 February 2003; revised manuscript received 28 April 2003; published 19 August 2003)

The compounds ZrW_2O_8 and HfW_2O_8 undergo large isotropic negative thermal expansion (NTE) over a wide range of temperatures up to 1443 K and 1050 K, respectively. We have showed previously that large softening of low-energy phonons in ZrW_2O_8 is responsible for its anomalous thermal expansion behavior. In order to understand the effect of replacing Zr by Hf on NTE behavior we report lattice dynamical calculations and neutron time-of-flight spectroscopic measurements of the phonon density of states for cubic HfW_2O_8. The calculated phonon spectrum for cubic HfW_2O_8 is in fair agreement with the experimental data. The phonon spectra in the Zr and Hf compounds differ at low energies largely due to the mass difference. The calculated negative thermal expansion for HfW_2O_8 is in good agreement with experimental data from the literature. We further report a calculation of the pressure dependence of the detailed phonon dispersion relation which reveals large softening of several phonon branches on compression associated with the NTE.

DOI: 10.1103/PhysRevB.68.054302 PACS number(s): 78.70.Nx, 63.20.Dj, 65.40.De

I. INTRODUCTION

The compounds ZrW_2O_8 and HfW_2O_8 are of considerable interest due to their large isotropic negative thermal expansion[1] (NTE) in their cubic phase over a wide range of temperatures up to 1443 K and 1050 K, respectively. This remarkable feature makes these compounds potential constituents in composites to adjust the thermal expansion to a desired value. These compounds exhibit a framework structure[1,2] which consists of the corner-sharing WO_4 tetrahedra and ZrO_6 (HfO_6) octahedra. At room temperature, these compounds crystallize in cubic structure (space group $P2_13$). There is no significant difference between the structures[2] of ZrW_2O_8 and HfW_2O_8. There is a disorder phase transition[1,3] at about 400 K (space group $Pa\bar{3}$).

The absolute value of the thermal expansion coefficient in HfW_2O_8 is found[3] to be lower in comparison to that in ZrW_2O_8. An analysis of specific heat data[4] for the two compounds suggests that the mass difference between the Zr and Hf would lead to differing distributions of the low-energy phonon modes in these compounds. Grúneisen parameters of the Raman-active phonons of energy above 5 meV have been estimated[5] in both the Zr and Hf compounds from high-pressure experiments. A model based on these estimates, however, yields[5(b)] a rather large volume thermal expansion coefficient in ZrW_2O_8 (of -45×10^{-6} K^{-1} at 300 K compared with the experimental value[1] of -29×10^{-6} K^{-1}). A similar model for HfW_2O_8 reproduces thermal expansion coefficient at room temperature[5(a)] but would not give satisfactory values at low temperatures.[6] It appears that a proper description of NTE requires consideration of both the acoustic and optic phonon modes in the entire Brillouin zone. Recently it has been suggested[7] that certain translational motion of WO_4 tetrahedra is responsible for NTE in ZrW_2O_8. We also note that a high-pressure neutron diffraction study of HfW_2O_8 shows a cubic-to-orthorhombic structural phase transition[2] (space group $P2_12_12_1$) at about 6 kbar. The orthorhombic phase also shows an anomalous negative thermal expansion behavior.[2]

Previously, we have shown[6,8–10] via lattice dynamical calculations and high-pressure inelastic neutron scattering experiments that a large softening of several low-energy phonons (up to 8 meV) is mainly responsible for the anomalous thermal expansion in ZrW_2O_8. Phonon density-of-states measurements[11] are available in ZrW_2O_8. In order to understand the effect on the NTE behavior due to the replacement of Zr by Hf, we have carried out a joint study of lattice dynamics calculations and phonon density-of-states measurements for HfW_2O_8. Section II gives details about the experimental technique. The details about the lattice dynamical calculations are given in Sec. III, while the results and discussion and conclusions are presented in Secs. IV and V, respectively.

II. EXPERIMENT

The polycrystalline sample of HfW_2O_8 is prepared from stoichiometric amounts of $HfOCl_2\cdot xH_2O$ (99% Wah Chang, Albany, Oregon, USA) and H_2WO_4 (98+ %, Alfa Aesar, Ward Hill, Massachusetts, USA). The $HfOCl_2$ is dissolved in water and mixed with the solution of H_2WO_4 in ammonium hydroxide. The precipitate is dried at 600 °C, heated to 1200 °C for 2 h, and quenched. The heating to 1200 °C is then repeated with intermittent grindings until the compound is found to be x ray pure.

The inelastic neutron scattering experiments were carried out using the High-Resolution Medium-Energy Chopper Spectrometer at the Intense Pulsed Neutron Source of Argonne National Laboratory. The spectrometer is equipped with a large detector bank covering a wide range ($-10°$ to 140°) of scattering angles. A polycrystalline sample of cubic HfW_2O_8 (25 g) was placed inside a sealed aluminum container. We have chosen a high incident energy (E_0 = 200 meV) of neutrons, which permits the data to be collected over a wide range of momentum transfer Q from 4 to 19 $Å^{-1}$. This is needed to ensure an effectively uniform

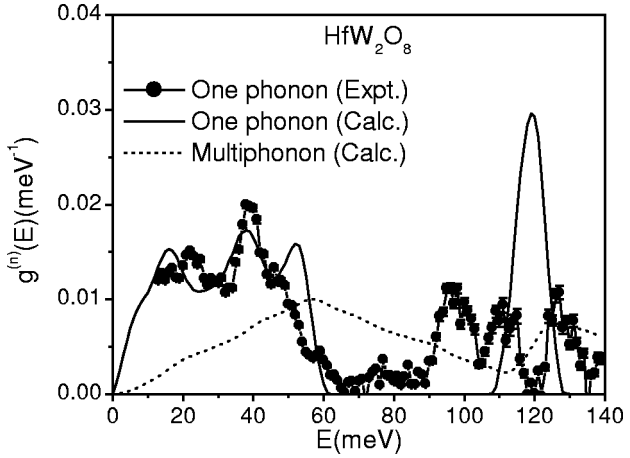

FIG. 1. The experimental and calculated neutron-weighted phonon density of states of cubic HfW_2O_8. In order to account for the experimental resolution broadening in the cubic phase the calculated spectrum has been convoluted with a Gaussian function of a full width at half maximum (FWHM) of 7 meV. The multiphonon contribution (dotted line) has been subtracted from the experimental data of the cubic phase to obtain the experimental one-phonon density of states.

sampling of Q wave vectors over the Brillouin zone, according to the incoherent approximation.[12] In order to reduce multiphonon scattering, the phonon measurements were carried out at low temperatures of 7 K. Background scattering was subtracted from the data by using an empty-container run. Measurements of the elastic incoherent scattering from a vanadium standard provided detector calibration and intensity normalization. The data were properly averaged over the range of scattering angles to obtain the neutron-cross-section-weighted phonon density of states $g^{(n)}(E)$ from the measured scattering function $S(Q,E)$ in the neutron energy loss experiments according to the incoherent approximation[12]

$$g^{(n)}(E)=A\left\langle \frac{e^{2W(Q)}}{Q^2}\frac{E}{n(E,T)+1}S(Q,E)\right\rangle \tag{1}$$

$$\simeq B\sum_p \frac{4\pi b_p^2}{M_p}g_p(E), \tag{2}$$

where $n(E,T)=[\exp(E/KT)-1]^{-1}$. Here, A and B are normalization constants, and b_p, M_p, and $g_p(E)$ are, respectively, the neutron scattering length, mass, and partial density of states of the pth atom in the unit cell. The factor $4\pi b_p^2/M_p$ for Hf, W, and O atoms is 0.057, 0.025, and 0.265 barns/amu, respectively. The quantity within $\langle\cdots\rangle$ represents an average over all Q values. $2W(Q)$ is the Debye-Waller factor.

III. LATTICE DYNAMICS

Neutron diffraction measurements show that there is no significant difference between the structures[2] of ZrW_2O_8 and HfW_2O_8. The precise structure of HfW_2O_8 has not been published. For these reasons, the potential parameters for

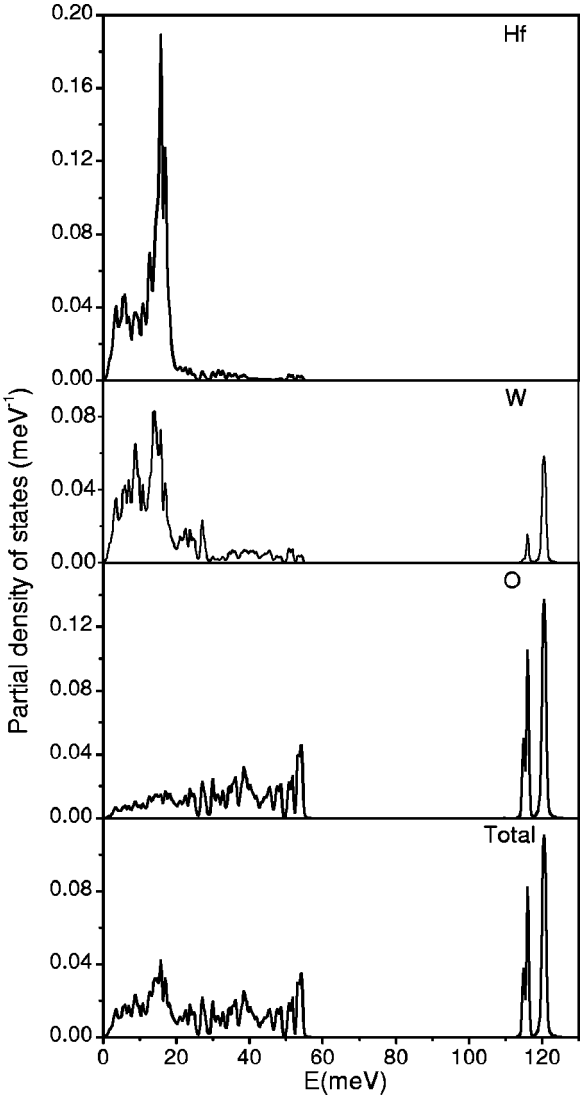

FIG. 2. The calculated partial density of states for various atoms and the total one-phonon density of states.

HfW_2O_8 were taken as the same as those for ZrW_2O_8 and could not be further optimized. The lattice dynamical calculations follow closely those for ZrW_2O_8 reported[6,8] previously. The semiempirical interatomic potential consists of Coulombic and short-ranged terms and a van der Waals attractive interaction between the oxygen atoms. Polarizibility of the oxygen atom has been introduced in the framework of the shell model.[13] The parameters of the interatomic potential are the effective charge and radius of the atoms. The charge and radius parameters are related to the ionic charge and radius of the atoms. The ionic radiis of zirconium (86 pm) and hafnium (85 pm) coordinated by six nearest oxygen atoms are essentially the same. This also justifies the use of the same interatomic potential[8] for HfW_2O_8 as that used previously for ZrW_2O_8. The phonon frequencies as a function of wave vectors in the entire Brillouin zone and its volume dependence under the quasiharmonic approximation are calculated using a computer program[14] developed by us.

In quasiharmonic approximation[13] the contribution from

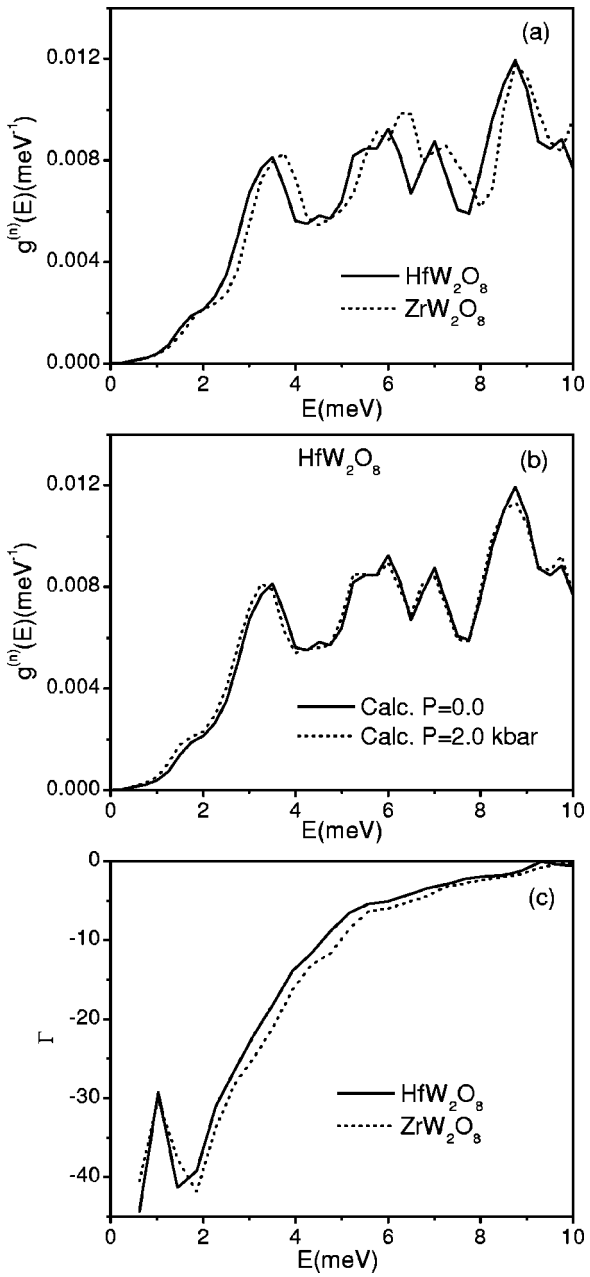

FIG. 3. (a) Comparison of the calculated phonon density of states at low energies between cubic ZrW_2O_8 and HfW_2O_8. (b) The neutron-cross-section-weighted phonon density of states below 10 meV at ambient pressure (solid line) and high pressure (dotted line) for cubic HfW_2O_8. The calculated curves have been broadened with a Gaussian function of a FWHM of 0.5 meV. (c) The calculated mode Grüneisen parameter $[\Gamma(E)]$ averaged over phonon of energy (E) for cubic HfW_2O_8 (solid line) and ZrW_2O_8 [dotted line (Ref. 8)].

each phonon mode of energy E_i to the volume thermal expansion coefficient is given by

$$\alpha_V = \frac{1}{BV}\Gamma_i C_{Vi}(T), \tag{3}$$

where Γ_i $(=-\partial \ln E_i/\partial \ln V)$ is the mode Grüneisen parameter, C_{Vi} is the specific heat of the phonon mode of energy

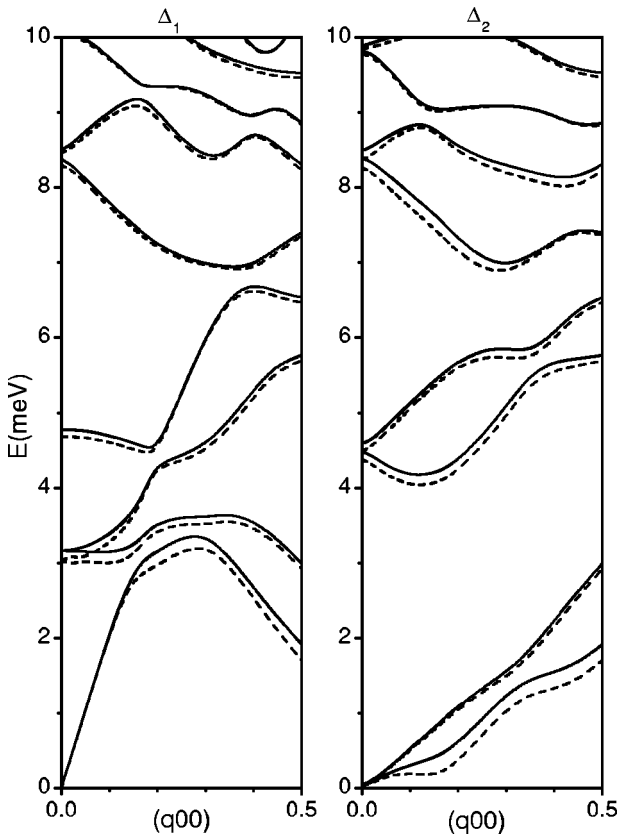

FIG. 4. The calculated phonon dispersion relation upto 10 meV for cubic HfW_2O_8 along the [100] direction. The solid and dashed lines correspond to ambient and 2.6 kbar.

E_i, B is the bulk modulus, and V is the unit cell volume. This procedure is applicable when the explicit anharmonicity of phonons is not very significant, and the thermal expansion arises mainly from the implicit anharmonicity, i.e., the change of phonon frequencies with volume. We have also included the contribution to thermal expansion arising from variation of the bulk modulus with volume.[15] The procedure is found to be satisfactory in our previous calculations[8,16–21] of ZrW_2O_8, $FePO_4$, aluminosilicate garnets, $MgSiO_3$, Mg_2SiO_4, $ZrSiO_4$, $LiYF_4$, $LiYbF_4$, and $MFX(M=\text{Ba, Pb, Sr};\ X=\text{Cl, Br,I})$. Due to the very large Debye temperatures in most of these systems, the quasiharmonic approximation seems to be suitable up to fairly high temperatures. Since C_{Vi} is positive for all modes at all temperatures, it is clear that the NTE would result only from large negative values of the Grüneisen parameter for certain phonons; the values should be large enough to compensate for the normal positive values of all other phonons. We have used the contribution of all 132 phonons at each wave vector on a $9\times9\times9$ mesh in an octant of the cubic Brillouin zone for calculations of phonon density of states and thermal expansion coefficient in the cubic phase.

IV. RESULTS AND DISCUSSION

A. Neutron inelastic scattering, total and partial phonon density of states, and phonon dispersion relation

The experimental and calculated neutron-weighted one-phonon densities of states as shown in Fig. 1 reveal a gap at

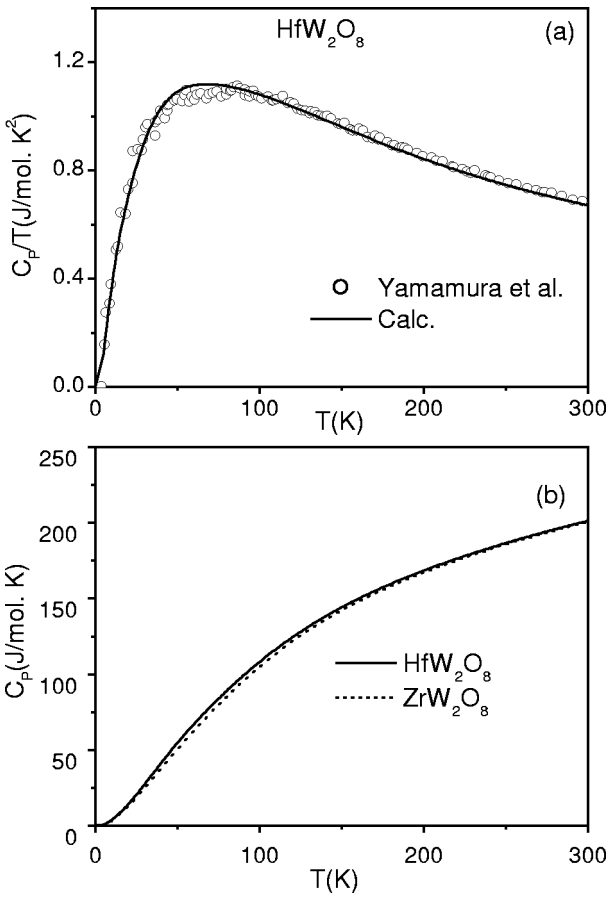

FIG. 5. (a) The calculated and experimental (Ref. 4) specific heat of cubic HfW_2O_8. (b) Comparison between the calculated specific heat of cubic HfW_2O_8 (solid line) and ZrW_2O_8 [dotted line (Ref. 8)].

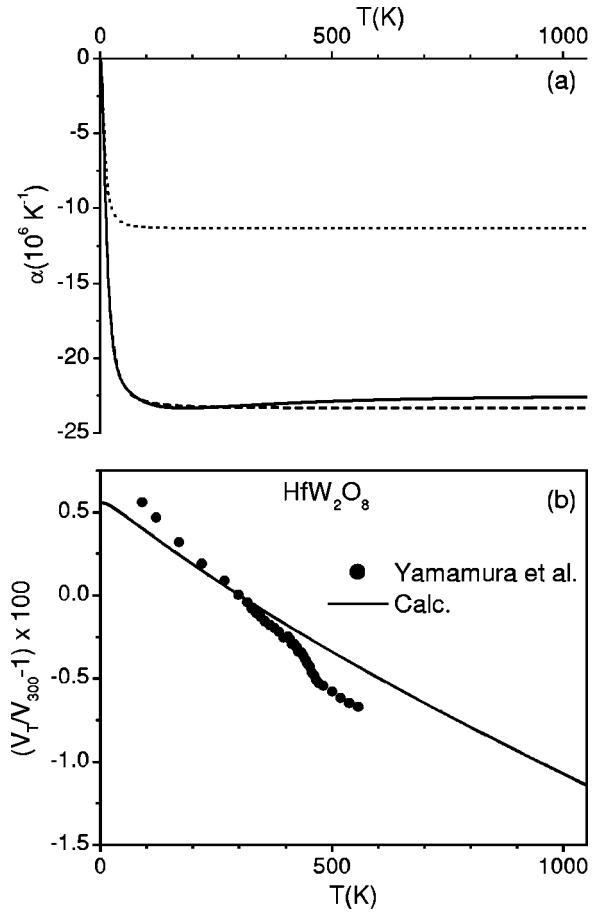

FIG. 6. (a) The calculated volume thermal expansion (solid line) in the cubic HfW_2O_8 along with separate contributions from the two lowest phonon branches (dotted line) and all the phonons below 8 meV (dashed line). (b) The experimental (Ref. 3) and calculated relative thermal expansion for cubic HfW_2O_8 $(V_T/V_{300}-1)\times 100\%$, V_T and V_{300} being the cell volumes at temperature T and 300 K, respectively. There is a small sharp drop in volume for cubic phase at about 400 K associated with a order-disorder phase transition. It is noted in Ref. 1(a) that the NTE in HfW_2O_8 continues until 1050 K; however, specific data were not given.

about 60–90 meV. Agreement between the experimental data and calculations below the gap is good. However, above 90 meV the calculated density of states shows a single peak around 120 meV, whereas the experimental data reveal a three-peak structure. The phonons above 90 meV involve W-O stretching vibrations. Their force field is apparently more dispersed than that described by the interatomic potential in the lattice dynamical model. As far as the phonon contribution to the NTE behavior is concerned, only the low-energy phonons are involved (as shown below). Therefore our model is able to correctly account for the thermal expansion behavior.

The calculated partial densities of states (Fig. 2) for the Hf atoms show an energy distribution extending only up to 60 meV, while the phonon vibrations due to W and O atoms contribute in the entire 140 meV range. Figure 3(a) shows a comparison of the phonon densities of states in Hf and Zr compounds. The significant larger mass of Hf (178.49) in HfW_2O_8 in comparison to Zr (91.22) in ZrW_2O_8 gives rise to a softening of the phonons at low energies. The lowest-energy peak in the phonon spectrum of cubic HfW_2O_8 occurs at 3.5 meV, as compared to 3.7 meV for the same peak in ZrW_2O_8.

The cubic phase has 44 atoms in the primitive cell and thus 132 phonon modes at each wave vector which are classified as $66\,\Delta_1+66\Delta_2$ along the [100] direction. The calculated pressure dependence of the phonon dispersion relation in cubic HfW_2O_8 along the [100] direction is shown in Fig. 4. We have plotted the phonon dispersion relation only up to 10 meV since phonons upto 8 meV are most relevant for understanding the negative thermal expansion behavior (as shown later). A large softening of phonons is observed in the cubic phase. The softening is very large for the lowest transverse acoustic mode in the group theoretical representation Δ_2 and also for a number of optic modes of energies lying between 3 and 8 meV in both the group theoretical representations. An elastic instability is found at a high pressure of about 3 kbar as revealed by the softening of the phonon mode (Fig. 4) at about $q=0.15$ along the [100] direction in the Δ_2 representation. The eigenvector of this mode indicates that the mode is close to a transverse acoustic vibration ac-

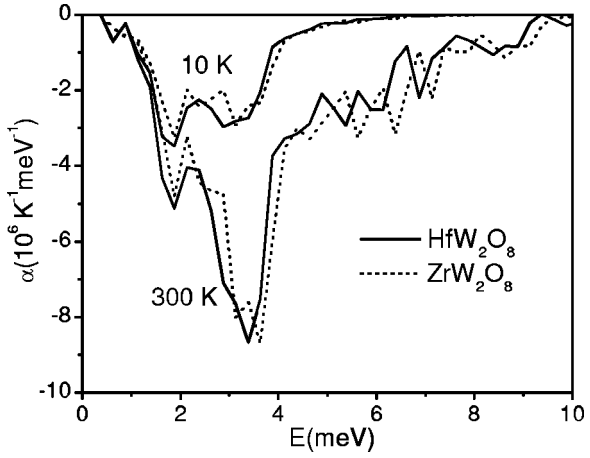

FIG. 7. The contribution of phonons of energy E to the volume thermal expansion as a function of E at 10 K and 300 K for cubic ZrW_2O_8 and HfW_2O_8.

companied by some internal angular distortions of the WO_4 tetrahedra. The calculated pressure dependence of the phonon spectrum [Fig. 3(b)] also shows that phonons below 8 meV soften in the cubic HfW_2O_8.

While Ref. 7 presents an interesting qualitative description of the negative thermal expansion in ZrW_2O_8 in terms of a certain vibrational mode, we find that a large number of phonon modes (Fig. 4) over the whole Brillouin zone show significant softening on compression of the lattice. Our model has been shown to lead to a quantitative description of the observed negative expansion. Reference 7 provides extended x-ray absorption fine structure (EXAFS) data on ZrW_2O_8, which indicate the relative bond strengths of the W-O, Zr-O, Zr-W, Zr-Zr, and W-W bonds. In particular, they note that WO_4 tetrahedra are essentially rigid, ZrO_6 are not as rigid, and W-Zr linkages are nearly as stiff as Zr-O. Our potential model includes an additional covalent term between W-O tetrahedral bonds only which ensures the rigidity of WO_4 tetrahedra. The calculated volume dependence of the structure shows that WO_4 tetrahedra behave like rigid units, while $HfO_6(ZrO_6)$ octahedra distort slightly.

B. Thermodynamic properties: Specific heat, Grüneisen parameter, and thermal expansion

The calculated one phonon density of states $g(E)$ is used to compute the specific heat. Figure 5(a) shows a comparison of the calculated specific heat with the available experimental data[4] in the cubic phase of HfW_2O_8. The good agreement between the calculated and experimental specific heats supports the correctness of the low-energy phonon density of states provided by the lattice dynamical model. The sharp increase in specific heat at low temperatures is due to a low-energy peak in the phonon spectrum at about 3.5 meV. We also compared in Fig. 5(b) the calculated specific heat of cubic HfW_2O_8 and ZrW_2O_8. At low temperature HfW_2O_8 has a larger specific heat. This is in agreement with the experimental[4] observations.

The calculated bulk modulus values of 88.4 GPa for cubic HfW_2O_8 is in good agreement with the experimental[2] value of 82 GPa. The calculated energy dependence of the Grüneisen parameter $\Gamma(E)$ for cubic HfW_2O_8 is shown in Fig. 3(c). The Grüneisen parameter has large negative values for phonons below 8 meV. In the 8–140 meV region $\Gamma(E)$ is small, varying within the range of -1 to 1. Figure 3(c) also shows the calculated[8] Grüneisen parameter for cubic ZrW_2O_8. The cubic HfW_2O_8 has lower values of $\Gamma(E)$ in comparison to ZrW_2O_8. This is consistent with the trend observed in the analysis of the thermal expansion and specific heat data.[4]

Our calculation of the temperature dependence of the volume thermal expansion coefficient [Fig. 6(a)] indicates that in cubic HfW_2O_8 phonon modes below 8 meV contribute to the NTE, among which the contribution from the two lowest phonon modes is about 40%. Similar behavior was calculated[8] for cubic ZrW_2O_8. The absolute value of thermal

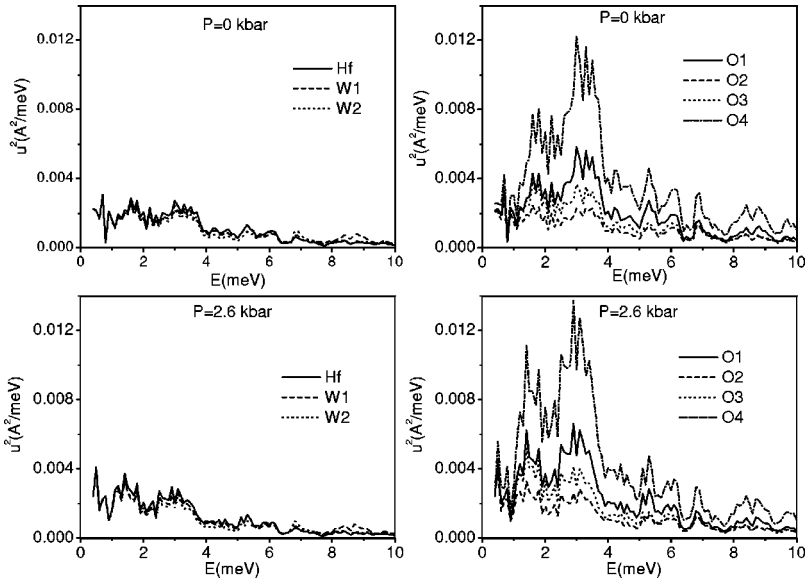

FIG. 8. The calculated contribution to the mean-squared amplitude of various atoms arising from phonons of energy E at $T=300$ K in the cubic HfW_2O_8 at ambient pressure and 2.6 kbar. The atoms are labeled as indicated in Refs. 1(a) and 8.

expansion coefficient for HfW_2O_8 is smaller in comparison with ZrW_2O_8. The comparison between the calculated and experimental data[3] for cubic HfW_2O_8 is shown in Fig. 6(b).

In Fig. 7 we show the contribution of various phonons to the thermal expansion as a function of phonon energy at 10 K and 300 K for cubic ZrW_2O_8 and HfW_2O_8. The maximum negative contribution to α_V at both temperatures is from the modes of energy from 3 to 5 meV. Similar behavior is calculated from the analysis of our high-pressure inelastic neutron scattering results[10] and diffraction data[22] for cubic ZrW_2O_8. At 10 K the contribution from modes above 5 meV is negligible. At high temperature (300 K) higher-energy modes are also populated and they start contributing to the thermal expansion.

The structure[1(a)] of HfW_2O_8 consists of a pair of WO_4 tetrahedra and HfO_6 octahedra. Two different tetrahedra are formed around W1 and W2 atoms. Three O1 and one O4 oxygen atoms are connected to W1, while three O2 and one O3 are connected to W2. The HfO_6 octahedra are formed by three O1 and three O2 atoms around Hf atoms. While O1 and O2 atoms link the WO_4 tetrahedra with HfO_6 octahedra, the oxygens O3 and O4 are connected only to W atoms of WO_4 tetrahedras. In order to understand the nature of the phonons responsible for NTE we have plotted (Fig. 8) the partial contributions of the phonons of different energies to the mean-square vibrational amplitude of the various atoms in HfW_2O_8. The modes up to 1 meV are largely acoustic in nature, but O4 atoms have larger amplitudes than other atoms. Above 1 meV, the O1 and O4 atoms connected to W1 have larger amplitudes in comparison with O2 and O3 connected to W2 atoms. Further, the various oxygen atoms constituting the tetrahedra have significantly different values of their vibrational amplitudes, which indicates distortions of the tetrahedra. Above 4 meV the amplitude of all the atoms is relatively small. The phonon modes of energy about 4 meV contribute (Fig. 7) a maximum to the negative thermal expansion. At high pressures the amplitudes of all the atoms increase by about 10%. This is mainly because of the increase in amplitude of the phonon modes of energy around 2 meV by 40% (Fig. 8). The distortions of WO_4 tetrahedra increase with compression.

V. CONCLUSIONS

Our lattice dynamical calculations produced a phonon spectrum for the cubic HfW_2O_8 that is in good agreement with the observed phonon spectrum at low energies and in fair agreement at high energies. The phonon spectra of Zr and Hf compounds differ at low energies mainly due to the mass difference. Like ZrW_2O_8 the major contribution to the thermal expansion in HfW_2O_8 originates from low-energy phonons. The calculated Grüneisen parameter at low energies for cubic HfW_2O_8 is lower than that for ZrW_2O_8. This results in a smaller value of negative thermal expansion coefficient in HfW_2O_8. These observations are in agreement with experimental data from the literature.[3,4] The calculations reveal that a large number of phonon branches in the dispersion relation undergo softening on compression which is associated with the negative thermal expansion in these compounds.

ACKNOWLEDGMENTS

Work performed at Argonne National Laboratory was supported by the U.S. DOE-BES under Contract No. W-31-109-ENG-38. We thank Wah Chang, Albany, Oregon for supplying $HfOCl_2 \cdot xH_2O$ for the preparation of HfW_2O_8.

[1] (a) T.A. Mary, J.S.O. Evans, T. Vogt, and A.W. Sleight, Science **272**, 90 (1996); J.S.O. Evans, T.A. Mary, T. Vogt, M.A. Subramanian, and A.W. Sleight, Chem. Mater. **8**, 2809 (1996); (b) It is noted in Ref. 1(a) that ZrW_2O_8 decomposes above 1050 K into ZrO_2 and WO_3 and that the components react again around 1380 K to reform ZrW_2O_8. A volume data at 1443 K (A.W. Sleight [unpublished work as cited by J.S.O. Evans, J. Chem. Soc. Dalton Trans. **19**, 3317 (1999)]) shows that the negative expansion continues until this temperature.

[2] J.D. Jorgensen, Z. Hu, S. Short, A.W. Sleight, and J.S.O. Evans, J. Appl. Phys. **89**, 3184 (2001).

[3] Y. Yamamura, N. Nakajima, and T. Tsuji, Phys. Rev. B **64**, 184109 (2001).

[4] Y. Yamamura, N. Nakajima, T. Tsuji, M. Koyano, Y. Iwasa, S. Katayama, K. Saito, and M. Sorai, Phys. Rev. B **66**, 014301 (2002).

[5] (a) B. Chen, D.V.S. Muthu, Z.X. Liu, A.W. Sleight, and M.B. Kruger, Phys. Rev. B **64**, 214111 (2001); J. Phys.: Condens. Matter **14**, 13 911 (2002); (b) T.R. Ravindran, A.K. Arora, and T.A. Mary, Phys. Rev. Lett. **84**, 3879 (2000); J. Phys.: Condens. Matter **13**, 11 573 (2002).

[6] S.L. Chaplot and R. Mittal, Phys. Rev. Lett. **86**, 4976 (2001).

[7] D. Cao, F. Bridges, G.R. Kowach, and A.P. Ramirez, Phys. Rev. Lett. **89**, 215902 (2002).

[8] R. Mittal and S.L. Chaplot, Phys. Rev. B **60**, 7234 (1999).

[9] R. Mittal and S.L. Chaplot, Solid State Commun. **115**, 319 (2000).

[10] R. Mittal, S.L. Chaplot, H. Schober, and T.A. Mary, Phys. Rev. Lett. **86**, 4692 (2001).

[11] G. Ernst, C. Broholm, G.R. Kowach, and A.P. Ramirez, Nature (London) **396**, 147 (1998).

[12] D.L. Price and K. Skold, in *Neutron Scattering*, edited by K. Skold and D.L. Price (Academic Press, Orlando, FL, 1986), Vol. A; J.M. Carpenter and D.L. Price, Phys. Rev. Lett. **54**, 441 (1985); S.N. Taraskin and S.R. Elliott, Phys. Rev. B **55**, 117 (1997).

[13] P. Bruesch, *Phonons*: *Theory and Experiments* (Springer, Berlin 1982), Vol. 1; G. Venkatraman, L. Feldkamp, and V.C. Sahni, *Dynamics of Perfect Crystals* (MIT Press, Cambridge, MA, 1975).

[14] S.L. Chaplot (unpublished).

[15] V.K. Jindal and J. Kalus, Phys. Status Solidi B **133**, 89 (1986);

R. Bhandari and V.K. Jindal, J. Phys.: Condens. Matter **3**, 899 (1991).
[16] R. Mittal, S.L. Chaplot, A.I. Kolesnikov, C.-K. Loong, O.D. Jayakumar, and S.K. Kulshreshta, Phys. Rev. B **66**, 174304 (2002).
[17] R. Mittal, S.L. Chaplot, and N. Choudhury, Phys. Rev. B **64**, 094302 (2001).
[18] S.L. Chaplot, N. Choudhury, S. Ghose, M.N. Rao, R. Mittal, and P. Goel, Euro. J. Mineral **14**, 291 (2002).
[19] R. Mittal, S.L. Chaplot, A. Sen, S.N. Achary, and A.K. Tyagi, Phys. Rev. B **67**, 013403 (2003).
[20] A. Sen, S.L. Chaplot, and R. Mittal, Phys. Rev. B **67**, 024304 (2001).
[21] S.L. Chaplot, R. Mittal, E. Busetto, and A. Lausi, Phys. Rev. B **66**, 064302 (2002).
[22] W.I. David, J.S.O. Evans, and A.W. Sleight, Europhys. Lett. **46**, 661 (1999).